2005 WSEAS Int. Conf. on ENVIRONMENT, ECOSYSTEMS and DEVELOPMENT, Venice, Italy, November 2-4, 2005 (pp232-237)

Numerical Investigation of Wake Formation Around a Conical Island in Shallow-Water Flows

RODRIGUEZ C.[1], SERRE E.[1], REY C.[1] and RAMIREZ H.[2]

[1]Laboratoire de Modélisation et Simulation Numérique en Mécanique – Génie des Procédés (MSNM-GP) UMR6181 CNRS / Université d'Aix Marseille III
La Jetée, Technopole de Château-Gombert, 38 rue Frédéric Joliot-Curie 13451, Marseille Cedex 20, FRANCE
http://www.L3m.univ-mrs.fr

[2]Instituto Mexicano del Petroleo
Eje Central Lázaro Cárdenas No 152 San Bartolo Atepehuacan CP 07730
MEXICO

Abstract: - A series of numerical experiments has been carried out in order to investigate recirculating shallow-water flows in the wake of a conical model island with gently sloping side of 8%. A semi-implicit finite-difference method for solving depth-averaged and three-dimensional shallow water equations, with the usual hydrostatic pressure assumption, have been used to simulate the flows. According to the value of the wake stability parameter *S*, two types of island wakes have been obtained, classified into "vortex shedding" and "steady bubble" types. Both models provide a good overall agreement with the experimental results. A vigorous vortex shedding type wake is obtained at S=0.06 in very close agreement with the experimental observations. For very shallow depths where the wake is stabilized by the bed friction, the 3D model demonstrated a closer agreement with the experimental results, consisting in a steady bubble type wake at S=0.5.

Key-Words: Shallow-water flows, islands wakes, numerical modelling

1 Introduction

Shallow water flows, where the horizontal length scales are much larger than the vertical depth-limited scales, occur in a range of environmental engineering problems like in coastal regions, estuaries and rivers [1]. When these flows go past an obstacle (headland, promontory or island), separation-like effects can induce the occurrence of large-scale eddies which have a dominant effect on mixing processes relevant to solute or sediment trapping.

In this work, we have focused on flows around islands which generate recirculation zones typical of shallow-water flows. These large-scale recirculation zones have been shown in satellite images and aerial photographs (seen for example in [2]) and can have a strong impact on long term implications for marina fauna as well as for the location of commercial fisheries and fish farms [3].

A model of conical island has been chosen because it represents a close approximation of natural depth varying bathymetry and vertical sided models. This island model has been experimentally investigated in [4, 5], and an experimental database is available to compare with. However, the complexity of these flows due to depth varying bathymetry of the island and the unsteady nature of the wake is not completely understood and represents a challenging problem for accurate numerical investigations.

Experiments with a steady current flow across vertical circular cylinders [6] have shown how wake formation is controlled by the stability parameter $S = c_f D_m / h$, where c_f is bottom friction coefficient, h is water depth and D_m is the diameter at mid-depth in the conical island case. The results suggest the existence of two critical values $S_{c1} \approx 0.20$ and $S_{c2} \approx 0.40$. For $S < S_{c1}$, vortices were shed periodically from the island in the manner of a Kármán vortex street wake. For $S_{c1} < S < S_{c2}$, the wake underwent a transition from vortex shedding to an unsteady bubble type flow with an instability growing downstream of a

recirculating bubble attached to the body. Finally for $S > S_{c2}$, the transverse disturbances ceased and the wake was characterized by a steady wake bubble with slowly recirculating flow.

For many years now, there have been numerous contributions to the numerical modelling of shallow water flows [4, 6-9]. Early models were in depth-averaged form due to computational limitations and these are indeed still popular. The vertical velocity variation has of course to be assumed, which may not be a severe limitation if the boundary layer is fully developed through the water depth; in particular, the bed friction coefficient has to be specified. However in the present flow, the boundary-layer thickness is generally less than the water depth and it is thus impossible to specify the bed friction without numerical modelling of the boundary layer.

Here we adopt a two and three-dimensional forms of the shallow water equations, while still making the assumption of hydrostatic pressure. This enables the boundary-layer development to be computed directly but does not allow realistic representation of separation in a vertical plane which depends on the complete pressure (hydrostatic plus non-hydrostatic). It is of considerable interest to know whether such a relatively efficient formulation will predict the complex wake formations due to a gently sloping obstacle at low subcritical Froude numbers.

In this paper, a series of numerical experiments has been conducted to investigate the shallow-water wakes of a conical model island of small slope of 8°. Instantaneous velocity maps provide information on the evolution, transport and relative scales of eddy structures within the flow, for different values from parameter of stability S. The mathematical formulations are considered in section 2. Geometrical and numerical modelling are detailed in sections 3 and 4, respectively. Numerical results are presented in section 5.

2 Mathematical formulations

The three-dimensional equations that describing the flow in estuarine embayments and coastal oceans, can be derived from the Navier-Stokes equations. After turbulent averaging and under the simplifying assumption that the pressure is hydrostatic, these equations are given by:

$$u_t + (u \cdot \nabla)\vec{\mathbf{U}} = -g\nabla h + \nabla^2(n_E u) + f_{cor} \cdot v \qquad (1)$$

$$v_t + (v \cdot \nabla)\vec{\mathbf{U}} = -g\nabla h + \nabla^2(n_E v) - f_{cor} \cdot u \qquad (2)$$

$$\frac{\partial u}{\partial x} + \frac{\partial v}{\partial y} + \frac{\partial w}{\partial z} = 0, \qquad (3)$$

where $\vec{U}(x,y,z,t)$ is the velocity vector and u, v and w are respectively the velocity components in the directions x, y (horizontal) and z (vertical). u_t defines the time derivative. $\eta(x, y, t)$ is the water surface elevation measured from the undisturbed water surface, g is the constant gravitational acceleration. f_{cor} is the Coriolis parameter defined by $f_{cor} = 2\,\Omega\sin(\phi)$, where Ω is the earth rotation and ϕ the latitude angular.

The coefficient of eddy viscosity ν_E is defined as the mixing length model, whose equation [8] is:

$$n_E = \left(l_h^4 \left[2\left(\frac{\partial u}{\partial x}\right)^2 + 2\left(\frac{\partial v}{\partial x}\right)^2 + \left(\frac{\partial v}{\partial x} + \frac{\partial u}{\partial y}\right)^2 \right] + l_v^4 \left[\left(\frac{\partial u}{\partial z}\right)^2 + \left(\frac{\partial v}{\partial z}\right)^2 \right] \right)^{1/2}, \qquad (4)$$

where the vertical length scale $l_v = \kappa(z\text{-}z_b)$ for $(z\text{-}z_b)/h < \lambda/\kappa$ and $l_v = h\lambda$ for $\lambda/\kappa < (z\text{-}z_b)/h < 1$, κ is the von Karman constant typically 0.41, $(z - z_b)$ is the distance from the wall, $h(x, y)$ is the water depth measured from the undisturbed water surface, λ is a constant (typically 0.09) and the horizontal length scale is defined by $l_h = \beta l_v$ (the constant β has to be determined experimentally). In the case of parallel (or nearly parallel) flow, eddy viscosity reverts to its standard boundary-layer form. With $l_h = l_v$, it reverts to its correct mathematical three-dimensional form (with negligible vertical velocity or $(u \approx v) > w$).

Integrating the continuity equation over the depth and using a kinematic condition at the free surface leads to the free surface equation.

$$\frac{\partial h}{\partial t} = -\frac{\partial}{\partial x}\left(\int_{-h}^{h} u\, dz\right) - \frac{\partial}{\partial y}\left(\int_{-h}^{h} v\, dz\right), \qquad (5)$$

where $h(x, y)$ is the water depth measured from the undisturbed water surface.

The boundary conditions at the bottom are given by expressing the bottom stress in terms of the velocity components. The bottom stress can be related to the turbulent law of the wall, using a Manning-Chezy formula such as:

$$n_E \frac{\partial u}{\partial z} = \frac{g\sqrt{u^2+v^2}}{Cz^2}u, \quad n_E \frac{\partial v}{\partial z} = \frac{g\sqrt{u^2+v^2}}{Cz^2}v, \qquad (7)$$

where *Cz* is the Chezy friction coefficient.

The free surface is considered here as a slip boundary $\partial u/\partial z = \partial v/\partial z = 0$

Vertically averaged shallow-water equations have been also considered by integrating vertically equations (1) and (2) from the bed $z=-h$ to the free surface $z=\eta$. By using the free surface equation (5) and the boundary conditions (6) and (7), and after standard approximations on the non-linear advective terms, one gets the two-dimensional, vertically averaged shallow-water equations.

$$U_t + (U\cdot\nabla)\vec{U} = -g\nabla h + \nabla^2(n_E U) + f_{cor}\cdot V + \frac{t_x{}^w}{H} - \frac{g\sqrt{(U^2+V^2)}}{Cz^2 H}U \qquad (8)$$

$$V_t + (V\cdot\nabla)\vec{U} = -g\nabla h + \nabla^2(n_E V) - f_{cor}\cdot U + \frac{t_y{}^w}{H} - \frac{g\sqrt{(U^2+V^2)}}{Cz^2 H}V \qquad (9)$$

$$\frac{\partial h}{\partial t} + \frac{\partial(HU)}{\partial x} + \frac{\partial(HV)}{\partial y} = 0\,, \qquad (10)$$

where $U = (1/H)\int_{-h}^{h} u\,dz$ and $V = (1/H)\int_{-h}^{h} v\,dz$ are the depth-averaged horizontal velocities, $\vec{U} = (U, V)$, and H is the total water depth, $H = h + \eta$.

3 Geometrical modelling

The conical island is located in the middle of a channel of 1.52 m wide by 4.52 m long, in order to avoid the disturbances caused by the boundary conditions (Fig. 1).

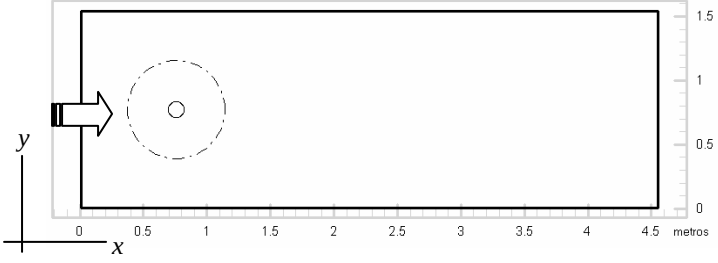

Fig. 1 Channel and island (the dashed line shows the island base

The bed is horizontal to correspond with experiments of [4]. In order to satisfy the hydrostatic assumptions, the conical island has a gently sloping side fixed at 8°.

Former studies of [4] have shown that the effect of this angle value on the wakes is small for (8° = α = 33.1°). The base is 0.75 m of diameter and the island centre is 0.76m from the upstream end.

4 Numerical modelling

Both 2D and 3D models use a second-order finite-difference scheme. The formulation is based on the semi-implicit Lagrangian scheme [10, 11]. In the Lagrangian description of the advected terms the total derivative for velocity is used, providing a low numerical diffusivity, and, although explicit, an unrestricted Courant condition.

The model computations were made with a horizontal square cell size of 0.0152 m (298 x 100) and a time step of 0.001s. For 3D simulations, the number of vertical cells was 10. Reducing the length of the mesh did not significantly affect the results.

The inlet boundary condition for the velocity is given by prescribing the value of the streamwise component $u = U_0$ at the inflow $x = 0$.

The outlet boundary condition is specified by Neuman's condition ($\partial u/\partial n = 0$). At the bottom and at the wall, the no-slip condition is applied, with a zero normal velocity component.

The code has been parallelized on a PC cluster and has used up to 6 non-overlapping rectangular subdomains. The cluster consists of 27 nodes bi-processors AMD Athlon: 2 nodes MP2000 / 1666MHZ (2 Go RAM, 4 discs SCSI of 80G0 in RAID5) and 25 nodes MP1800+/1525MHZ.

5 Results

Numerical experiments have been carried out for five values of the stability parameter *S* ranging between 0.06 and 0.8. The flow parameters are given in table 1.
In all cases, the water depth is less than the island height, and the the flow is subcritical (Froude number $(U_0/(gh)^{1/2}) < 0.3$).

Depth-averaged velocity vector plots produced by the 2D model are presented in fig. 2. The vector field shows an area of the computational domain close to the island.

	Case 01	Case 02	Case 03	Case 04	Case 05
S	0.06	0.27	0.4	0.5	0.8
h(m) ´ 10^3	45	20	14.8	14.8	14.8
U_0 (m/s)	0.115	0.1	0.1	0.1	0.1
Cz	55.33	48.04	45.93	41.35	32.69
c_f ´ 10^4	64	85	93	115	184
D_m (m)	0.429	0.608	0.645	0.645	0.645
Q ´ 10^4 (m^3/s)	79	30	22	22	22

Table 1 Summary of experimental conditions

For a low value of the stability parameter S=0.06, vortices are shed periodically from the island in the manner of a Kármán vortex street behind a vertical cylinder (Fig. 2a). Computations have then been performed at larger values of S. As the flow depth decreases in these experiments, both the magnitude of the bed friction coefficient c_f and the effective diameter of the island D_m increase (Table 1). Previous experimental studies [4, 6] identified a transition from a vortex shedding to an unsteady bubble wake: for the flows behind a conical island (S=0.40) [4] and behind a circular cylinder (0.20<S<0.50) [6]. Increasing S up to S=0.50, regular vortex shedding remains and the unsteady bubble flow has never been observed (Figs. 2b, c). Although this result is not in agreement with experimental observations it is similar to all the numerical solutions that we have found in the literature [4, 6-9].

The size of the rolled-up vortex has increased with S while it contains lower velocity. The apparent origin of the vortex shedding has moved further downstream relative to S=0.06. Consequently, in the near wake region, the flow velocity becomes lower when increasing S to 0.50, involving a weaker mixing process. At S=0.80, any form of well-organized vortex shedding ceased to exit confirming the stabilizing effect of the bed friction on the island wakes. The wake appears now as a steady bubble flow, in agreement with the experimental observations [4, 6]. This consisted of a bubble region with two zones of opposite recirculation attached to the island. The flow returns along the wake centerline from a distance of up to 0.90m downstream of the island center. The maximum velocity of the return flow is about 0.149U_0.

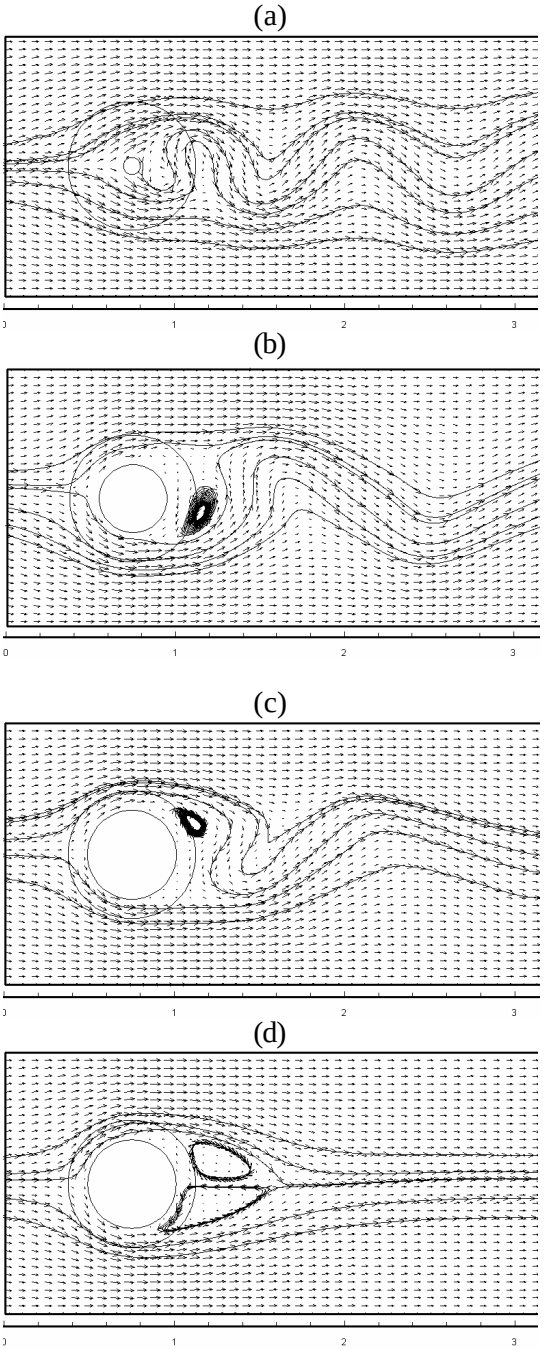

Fig. 2 Instantaneous depth-averaged velocity vector fields (2D model) and streamlines (black lines): S=0.06 (a), S=0.27 (b) S=0.5 (c) and S=0.8 (d).

Results from the 3D model are qualitatively very similar to those obtained with the 2D model. Although the plots in Fig. 3 are note exactly reproduced at the same time, there is a good agreement between the numerical results and the experimental observations of [4] for the vortex size as well as for the position of the dominant vortex center (Fig. 3a). As previously, the bed friction begins to alter the vortex shedding characteristics in the near wake as it has already been seen with S=0.27 (Fig. 2b). Nevertheless, the critical value of S, S=0.5, from which the

transverse disturbances cease (Fig. 3c) is in a much better agreement with experimental measurements [4] than using the 2D model. Indeed, the velocity field predicted by the 2D model at S=0.5 still shows a vigorous vortex shedding in the wake (Fig. 1c).

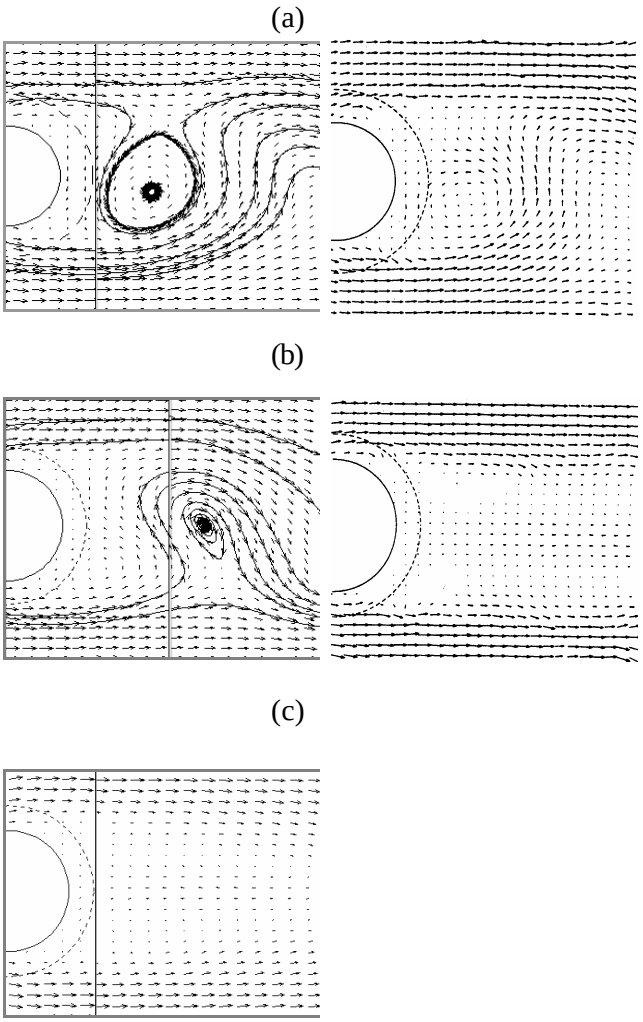

Fig. 3 3D simulation (on the left) and experimental [4] (on the right) velocity vector fields at the free surface: (a) S=0.27, (b) S=0.40 and (c) S=0.50.

Comparison between velocities time histories for both numerical models is shown in Fig. 4. The measuring position is 0.645m downstream of the island center and 0.82m from the wake centreline. The shedding period remains roughly the same using the 2D or 3D model, except at S=0.5 where the 3D flow becomes steady. The time period is of T=12s at S=0.06 and it increases up to T=20s for all the other values of S, ranging between 0.27-0.4 (3D) and 0.27-0.5 (2D). From Fig. 4 it is clear that the vigour of the oscillations is reduced in the 2D model relative to the 3D one. Moreover, the amplitude of the signal decreases when increasing S confirming the stabilizing effect due to the increase of the bed friction. Although the 3D model produces a more periodic and organized system than in experiments [4], velocity magnitude are roughly the same.

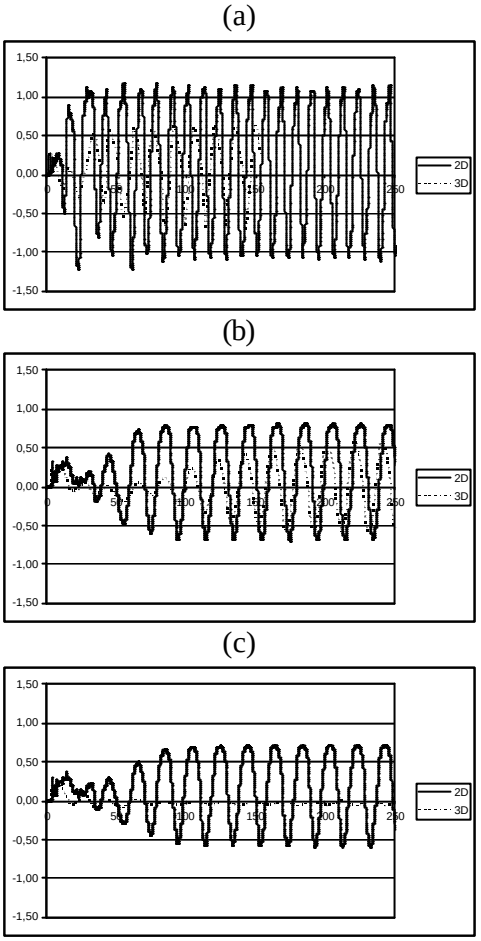

Fig. 4 Time history of v using 2D and 3D numerical models: (a) S=0.06, (b) S=0.40 and (c) S=0.50.

6 Concluding remarks

The main purpose of this paper was to establish a firm mathematical foundation for the numerical scheme and computational parallel algorithm for the numerical solutions of two and three-dimensional shallow-water flows. To this end, only the special case of constant density flow was considered.

A series of numerical experiments has been conducted to investigate the shallow recirculating flow in the wake of a conical model island with a gently sloping side of 8°. For small values of the wake stability parameter S<0.5 (3D model) and S<0.8 (2D model), the solutions exhibit well-organized vortex-shedding in the wakes island. For larger values of S, bed friction can act to suppress development of vortex shedding, and a steady bubble flow has been obtained with both

numerical models. Although 2D model gives a good qualitative comparison with experimental results [4, 6], 3D model gives better results especially when the bed friction was relatively large (S>0.4). It seems consequently that the velocity variations across the depth have to be represented when modelling flows for large values of S.

According to these good results, it is possible to be affirmed, that our numerical modelling is capable of reproducing the general features of a range of complex wake flows observed experimentally for oscillatory shallow-water flows around conical islands of small slope. These results encourage us to considered more complex oscillatory flows.

Three-dimensional computations are already in progress in order to investigate currents in the Gulf of Mexico. Numerical investigations of three-dimensional flow problems will not be complete without proper representations of transport of salt, variations in density distributions, and coupling of salt transport through baroclinic forcing. These aspects will be addressed in this future work.

Acknowledgement

Support for C.R.C. through CONACYT (Consejo Nacional de Ciencia y Tecnologia Mexico) is gratefully acknowledged. The authors would like to thank U. D'Ortona for fruitful discussions. Thanks also to D. Fougère and S. Fayolle for supporting computations performed on the PC cluster "Choeur" in the MSNM-GP laboratory.

References

[1] Jirka, G.H., Large scale structures and mixing processes in shallow flows, *J. Hydraul. Res.* Vol.39, 2001, pp. 567-573.

[2] Wolanski, E., Imberger, J. and Heron, M. L., Island wakes in shallow coastal waters, *J. Geophys. Res.*, Vol.89, 1984, pp. 10553-10569.

[3] Hartnett, M., Water quality aspects of offshore fish farming, *Proc. Instn. Civ. Engrs. Wat. Marit. and Energy*, Vol.101, 1993, pp.14521-14533.

[4] Lloyd, P. M. and Stansby, P. K., Shallow-water flow around model conical island of small side slope I: Surface-piercing, *J. Hydraul. Engng* ASCE Vol.123, 1997, pp. 1057-1068.

[5] Lloyd, P. M. and Stansby, P. K., Wake formation around islands in oscillatory laminar shallow-water flows. Part 1. Experimental investigation, *J. Fluid Mech*., Vol.429, 2001, pp. 217-238.

[6] Chen, D. and Jirka G. H., Experimental study of plane turbulent wakes in shallow water layer, *Fluid Dyn. Res*., Vol.16, 1995, pp. 11-41.

[7] Stansby, P. K., and Lloyd, P. M., Wake formation around islands in oscillatory laminar shallow-water flows. Part 2. Three-dimensional boundary layer modelling, *J. Fluid Mech*., Vol.429, 2001, pp. 239-254.

[8] Stansby, P. K., A mixing-length model for shallow turbulent wakes, *J. Fluid Mech*., Vol.495, 2003, pp. 369-384.

[9] Serre, E., Stansby, P., Laurence, D. and Launder, B. E., Ecoulement autour d'un modèle d'île conique en eau peu profonde, *Rev. Eur. Eléments Finis*, Vol.12, No(2-3), 2003, pp. 361-371.

[10] Casulli, V. and Cheng, R., Semi-implicit finite difference methods for three-dimensional shallow water flow, *International Journal for Numerical Methods in Fluids*, Vol.15, 1992, pp. 629-648.

[11] Casulli, V., Semi-implicit finite difference methods for the two-dimensional shallow water equations, *J. Computational Phys*., Vol.86, 1990, pp. 56-74.